The Human Trithorax Protein hASH2 Functions as an Oncoprotein

Juliane Lüscher-Firzlaff,[1] Isabella Gawlista,[1] Jörg Vervoorts,[1] Karsten Kapelle,[1] Till Braunschweig,[2] Gesa Walsemann,[1] Chantal Rodgarkia-Schamberger,[3] Henning Schuchlautz,[1] Stephan Dreschers,[1] Elisabeth Kremmer,[4] Richard Lilischkis,[1] Christa Cerni,[3] Axel Wellmann,[2] and Bernhard Lüscher[1]

[1]Institut für Biochemie and [2]Institut für Pathologie, Klinikum, RWTH Aachen University, Aachen, Germany; [3]Institut für Krebsforschung, Klinik für Innere Medizin I, Medizinische Universität Wien, Wien, Austria; and [4]GSF-Institut für Molekulare Immunologie, Munich, Germany

Abstract

Regulation of chromatin is an important aspect of controlling promoter activity and gene expression. Posttranslational modifications of core histones allow proteins associated with gene transcription to access chromatin. Closely associated with promoters of actively transcribed genes, trimethylation of histone H3 at lysine 4 (H3K4me3) is a core histone mark set by several protein complexes. Some of these protein complexes contain the trithorax protein ASH2 combined with the MLL oncoproteins. We identified human ASH2 in a complex with the oncoprotein MYC. This finding, together with the observation that hASH2 interacts with MLL, led us to test whether hASH2 itself is involved in transformation. We observed that hASH2 cooperates with Ha-RAS to transform primary rat embryo fibroblasts (REF). Furthermore, transformation of REFs by MYC and Ha-RAS required the presence of rAsh2. In an animal model, the hASH2/Ha-RAS–transformed REFs formed rapidly growing tumors characteristic of fibrosarcomas that, compared with tumors derived from MYC/Ha-RAS transformed cells, were poorly differentiated. This finding suggests that ASH2 functions as an oncoprotein. Although *hASH2* expression at the mRNA level was generally not deregulated, hASH2 protein expression was increased in most human tumors and tumor cell lines. In addition, knockdown of hASH2 inhibited tumor cell proliferation. Taken together, these observations define hASH2 as a novel oncoprotein. [Cancer Res 2008;68(3):749–58]

Introduction

The development of a tumorigenic cell is a complex multistep genetic process that results in the deregulation of fundamental aspects of cell physiology, including proliferation, differentiation, and apoptosis (1). In recent years, RNA expression profiling was instrumental to identify genes that are deregulated in tumor cells and thus potentially relevant for tumor development and progression (2). In addition, comparative genomic hybridization on a global scale allowed the identification of DNA regions that are either underrepresented or overrepresented in distinct tumors (3). These studies revealed novel oncogenes and tumor suppressor genes that are deregulated or genetically altered in human malignancies. However, some oncogenes and tumor suppressor genes cannot be depicted by these methods. This is true for cases in which proteins are deregulated as a result of small mutations or because of deregulated cellular signaling that affects the function of the respective proteins (4, 5). Linking such proteins with tumor development and/or progression requires, in general, functional assays.

The *polycomb group* (PcG) and *trithorax group* (TrxG) genes were originally identified in *Drosophila*, where the products of these genes are intimately involved in the segmentation of the embryo (6). The expression pattern of *hox* genes, initially defined by *gap* and *pair-rule* genes, is maintained after gastrulation by the activities of *PcG* and *TrxG* gene products. In general, although the PcG proteins are responsible to maintain the repressed status of distinct *hox* genes, the TrxG proteins perpetuate the transcribed status of these genes (7, 8). PcG and TrxG proteins assemble into large protein complexes that control gene transcription, at least in part, by modulating chromatin. The TrxG gene *ash2* (*absent, small*, or *homeotic discs 2*) was discovered in a screen for lethality during the late larval/early pupal stage of *Drosophila* development with imaginal disc defects (9). Mutations of Ash2 cause homeotic transformations in many segments of *Drosophila* and, additionally, result in a variety of pattern formation defects (10). Loss of Ash2 inhibits *hox* gene expression, consistent with a function of Ash2 as a TrxG protein associated with maintaining the expression of *hox* genes (11). Furthermore, array analyses revealed many additional targets controlled by Ash2, including genes involved in cell cycle and cell proliferation control (12, 13). These findings suggest that Ash2 is not only involved in regulating aspects of tissue development but also controls functions associated with cell proliferation in the adult.

The molecular analysis showed that mammalian ASH2 is a component of protein complexes of various composition, some including mixed-lineage leukemia (MLL) oncoproteins, that contain histone methyltransferase (HMT) activity (14–20). Recent findings have shown that these complexes trimethylate (me3) histone H3 at lysine 4 (H3K4; refs. 21–23). H3K4me3 is one of a large number of distinct modifications that have been identified on core histones and are part of elaborate mechanisms that evolved to control the structure and the chemical surface of chromatin (24, 25). These modifications control the access of proteins to nucleosomes that, in turn, regulate various aspects associated with gene transcription, including chromatin remodeling and the activities of transcriptional regulators and polymerase complexes (26). H3K4me3 is a histone mark that is closely associated with transcribed genes (22, 25, 27). Several recent studies have shown

Note: J. Lüscher-Firzlaff and I. Gawlista contributed equally to this work.

Current address for G. Walsemann: PAREXEL International GmbH, Am Bahnhof Westend 11, 14059 Berlin, Germany. Current address for R. Lilischkis: BTF Precise Microbiology, 35-41 Waterloo Road, North Ryde Sydney, NSW 2113, Australia. Current address for A. Wellman: Institut für Pathologie, Siemensplatz 4, 29223 Celle, Germany. C. Cerni is deceased.

Requests for reprints: Bernhard Lüscher, Institut für Biochemie, Klinikum, RWTH Aachen University, Pauwelsstrasse 30, 52057 Aachen, Germany. Phone: 49-241-8088850; E-mail: luescher@rwth-aachen.de.

doi:10.1158/0008-5472.CAN-07-3158

that H3K4me3 is found within the 5′ region (i.e., the proximal promoter) of virtually all active genes. In addition, this modification correlates strongly with the presence of active polymerase II (28–32). The proteins that can read H3K4me3 include members of the ING family that associate with chromatin remodeling activity and with histone acetyl transferases (33). Furthermore, the TAF3 subunit of the basal transcription factor complex transcription factor IID interacts with H3K4me3, thereby enhancing polymerase II recruitment (34). In addition, the JMJD2A demethylase also associates with H3K4me3 (35). Together, these findings suggest that trimethylation of H3K4 is an important modification of active chromatin that is strongly associated with gene transcription.

Recently, we identified several proteins associated with the oncoprotein MYC in a human T-cell tumor line (36). Microsequencing of the protein species with an apparent molecular weight of 86 kDa revealed its identity as human ASH2. This finding suggested that ASH2 might be involved in transformation. Therefore, we tested for the transforming activity of ASH2 using the rat embryo fibroblast (REF) cotransformation assay (37). We found that ASH2 cooperates efficiently with an activated Ha-RAS. Furthermore, knockdown of rAsh2 inhibited transformation by MYC and Ha-RAS. The ASH2/Ha-RAS–transformed REFs formed rapidly growing, poorly differentiated tumors in animals. Interestingly, the analysis of ASH2 in human tumors revealed that the *ASH2* gene is not overexpressed, but that, in general, the protein is present at increased levels. Knockdown of ASH2 interfered with the proliferation of tumor cell lines. Together, these findings suggested strongly that ASH2 possesses oncogenic activities and that its expression is relevant for tumor cell proliferation.

Materials and Methods

Cells and transformation assays. All human cell lines were cultured as recommended by the American Tissue Culture Collection. Human diploid fibroblasts (HDF; obtained from J. Baron, Department of Dermatology, RWTH, Aachen, Germany) were grown in DMEM supplemented with 10% FCS and human mammary epithelial cells (HMEC) in MEGM CC-3051 medium (Clonetics). Peripheral blood mononuclear cells were obtained from the blood bank of the RWTH Aachen University Medical School. Human tumor cell lines were transfected using ExGen500 as recommended by the manufacturer (MBI-Fermentas). REFs were obtained from 15.5-gestation-day-old Fischer rat embryos by fractionated trypsinization as described previously (38). REFs were grown in phenol red–free DMEM (Life Technologies) with 10% low-estrogen FCS (Bioconcept) and transfected with 2.5 μg of expression plasmids encoding the respective oncoproteins, 5 μg of pSUPER plasmids, and 1 μg of pRSVneo per 60-mm Petri dish using the calcium phosphate technique. Foci were stained and counted 14 days later. Transformed hASH2/Ha-RAS clones were selected in 200 μg/mL G418 (Geneticin, Life Technologies). MYC/Ha-RAS, E1a/Ha-RAS, and p53m/Ha-RAS clones were established previously (38). For proliferation assays, cells were cotransfected with pSUPER constructs and pBABE-puro and selected in the presence of puromycin (2 μg/mL) for 24 h. The cells were then washed and cultivated for an additional 4 to 5 days before staining with methylene blue (2 mg/mL methanol). Bromodeoxyuridine (BrdUrd) incorporation was measured in cells cotransfected with pSUPER constructs and pEGFP (ratio 15:1). The cells were pulse labeled with BrdUrd for 1 h before harvesting 72 h after transfection. The cells were then fixed, treated with DNaseI, and the incorporated BrdUrd was detected by indirect immunofluorescence (anti-bromodeoxyuridine antibody; Boehringer Mannheim). The number of BrdUrd-positive cells was determined relative to the number of transfected cells.

Plasmids. A PCR-amplified cDNA encoding hASH2 was cloned into an expression vector by standard procedures and sequenced. DNA oligonucleotides containing sequences corresponding to short interfering RNAs (siRNA) were cloned into the pSUPER vector (39). The following sequences were used: siRNA-hASH2, 5′-GGATCTCACTTACCGCCCT-3′; siRNA-rAsh2, 5′-CCCTAGCAGATCCATGCTT-3′; siRNA-rAsh2m, 5′-CCCTGCAGATCCATGCTT-3′; siRNA-rc-Myc, 5′-ATCCTGTACCTCGTCCGAT-3′; siRNA-rc-Mycm, 5′-ATCCTGTATCGTCCGAT-3′; siRNA-hSKP2, NT8 (see ref. 40). The different specific siRNA constructs reduced the relevant mRNA levels to 15% or less (data not shown). Expression vectors encoding human MYC, Ha-RAS, adenoviral E1a, and mutant p53 have been described previously (38). pBABE-puro and the expression vector for $p27^{KIP1}$ were obtained from G. Evan (University of California San Francisco, San Francisco, CA) and R. Bernards (Netherlands Cancer Institute, Amsterdam, The Netherlands), respectively.

Animal experiments. Seven-day-old male Fisher rats received s.c. injections of 5×10^4 transformed cells in PBS. Tumor size was monitored regularly, and the animals were killed by cervical dislocation when tumor diameters were ~20 mm for younger and 40 mm for older rats or before an unfavorable tumor localization would have restricted the rats' comfort. The animal experiment was performed according to the animal experiment approval GZ 66.009/98-Pr/4/00 given by the Austrian Ministry of Culture and Education. Similarly, BALB/c nude mice were injected s.c. with tumor cells, and tumor progression was monitored as above (Bezirksregierung Köln, 50.203.2-Ac36, 14/06).

Protein analysis. Western blot analyses were performed on whole-cell lysates in Frackelton buffer of exponentially growing cells (41). Monoclonal antibodies (mAb) 4C5 and 6A9 were generated by immunizing a LOU/C rat with bacterially expressed glutathione *S*-transferase–hASH2(1–444) fusion protein.

RNA analysis. Northern blot analyses were performed as described previously (41). A commercially available multitissue Northern blot was used (Clontech). The cancer profiling array (BD Bioscience) was obtained from E. Dahl (Institute of Pathology, RWTH, Aachen, Germany). For sequencing and real-time PCR analysis, RNA isolated by Trizol Reagent (Invitrogen) or RNeasy (Qiagen; tissue culture cells) was transcribed into cDNA using the Transcriptor First Strand cDNA Synthesis kit (Roche) as recommended. ASH2-specific cDNA was amplified (forward primer, 5′-GATGGCGGCGGCAGGAGC-3′ and reverse primer, 5′-GTGGGGAGAAAATGGTGAAAGGCAGG-3′), purified, and sequenced. Quantitative PCR was performed with the LightCycler FastStart DNA MasterSYBR Green I (Roche) or the QuantiTect SYBR Green PCR kit with a QuantiTect Primer Assay for hASH2 (Qiagen). The expression of *β-glucuronidase* was used for internal control in all experiments (forward primer, 5′-CTCATTTGGAATTTTGCCGATT-3′ and reverse primer, 5′-CCGAGTGAAGATCCCCTTTTTA-3′).

Microdissection. Frozen sections of tumors were processed for H&E staining. Normal and tumor tissue was identified microscopically. Ten adjacent 16-μm-thick frozen sections were mounted; the different regions of the tissue were marked, scraped off with a scalpel, and collected for Trizol reagent extraction (Invitrogen) according to the manufacturer's recommendations. The extracted tissue corresponded to roughly 50,000 cells per sample.

Immunohistochemistry. Sections of archived tumor samples as formalin-fixed, paraffin-embedded tissue were deparaffinized in xylene and rehydrated over ethanol and deionized water. Endogenous peroxidases were blocked by treating with 3% H_2O_2 in PBS for 15 min. Antigen demasking was performed in citrate buffer (pH 6.0) at 130°C for 10 min. Then, the samples were blocked in 1% fat-free milk powder and 10% horse serum in PBS. The specific staining was done using culture supernatant of mAb 4C5 and 6A9 diluted 1:200 in 1% fat-free milk powder in PBS at 37°C for 1 h. Biotinylated secondary anti-rat antibodies (1:500; Dianova) were incubated on the washed sample at 37°C for 30 min. Further incubation with avidin-biotin-peroxidase complex was performed as indicated by the manufacturer (Vectastain kit PK6100 Standard; Vector Laboratories). The staining of sections was performed with 3,3′-diaminobenzidine followed by counterstaining and coverslipping.

Results

Human ASH2 cooperates with HaRAS in transforming REFs. Previously, we identified novel interaction partners of the

oncoprotein MYC, including PARP10, nucleolin, and a protein with an apparent molecular mass of 86 kDa (36). Sequencing of tryptic peptides revealed that the p86 protein is the human orthologue of the *Drosophila* Ash2 protein (data not shown). A detailed account of the interaction of ASH2 with MYC will be described elsewhere. The finding that ASH2 interacts with MYC and the identification of ASH2 in protein complexes that contain the oncoprotein MLL1 or MLL4 prompted us to test whether hASH2 affects MYC/Ha-RAS–dependent transformation of REFs. Coexpression of hASH2 led to a mild increase in the number of foci (Fig. 1*A*). In contrast, knockdown of rat Ash2 (rAsh2) significantly inhibited foci formation (Fig. 1*A*). This effect was specific because siRNA constructs expressing a mutated version of the rAsh2-specific oligonucleotide had no effect (Fig. 1*A*). Furthermore, knockdown of rAsh2 did not interfere with E1a/HaRAS and mutant p53/HaRAS transformation of REFs (Fig. 1*C* and *D*). These findings suggested that rAsh2 was pivotal for cMYC/HaRAS-dependent transformation.

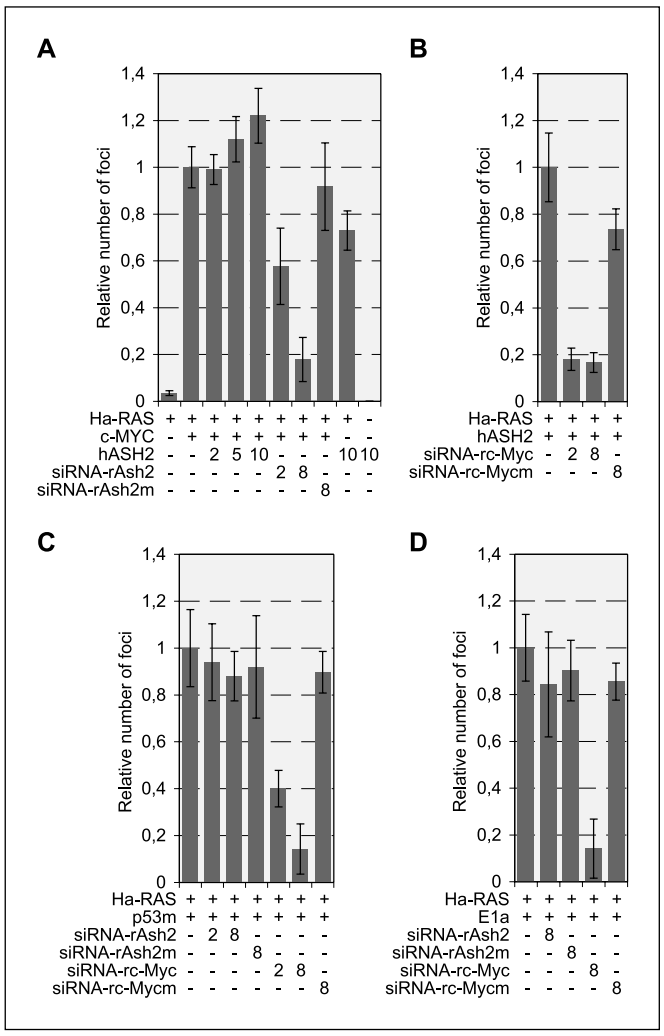

Figure 1. hASH2 cooperates with Ha-RAS to transform REF. *A* to *D,* REFs were cotransfected with expression plasmids encoding the indicated proteins and with pSUPER constructs expressing siRNAs that target the indicated mRNA. *m,* a mutated version of the targeting sequence. The empty pSUPER vector was cotransfected for control in these experiments. *Columns,* mean of at least two experiments with six individual plates per plasmid combination; *bars,* SD. For c-MYC/Ha-RAS, a single plate contained between 50 and 70 foci (*A*); for hASH2/Ha-RAS, between 35 and 50 foci (*B*); for mutant p53/Ha-RAS, between 40 and 50 foci (*C*); and for E1a/Ha-RAS, between 100 and 150 foci (*D*).

We also cotransfected expression constructs for hASH2 and Ha-RAS. Surprisingly, hASH2 was capable to cooperate with Ha-RAS in transforming REFs (Fig. 1*A*). The number of foci obtained with hASH2/Ha-RAS was ~70% of that observed for MYC/Ha-RAS–transformed cells. Thus, hASH2 behaved as an oncoprotein in the REF assay. To evaluate whether rat Myc was required for hASH2/Ha-RAS transformation, knockdown experiments were performed. Repression of rat Myc strongly inhibited hASH2/Ha-RAS but also E1a/Ha-RAS and mutant p53/Ha-RAS transformation (Fig. 1*B–D*). Together, these findings suggested that hASH2 has oncogenic properties in the REF cotransformation assay.

hASH2/HaRAS transformed REFs form tumors in animals. To further assess the transformed phenotype of the hASH2/Ha-RAS cells, two clones, AR-925 and AR-932, were established from individual foci. We were unable to generate lines from REF transfected with either hASH2 or Ha-RAS alone, indicating that neither of these two proteins was sufficient to immortalize primary cells. Both hASH2/Ha-RAS clones grew readily in culture and displayed a transformed morphology with refractile, spindle-like cells (data not shown). Both lines were then engrafted into syngeneic rats, and the growth of the cells was monitored. In five of five and four of five animals injected with AR-925 or AR-932 cells, respectively, tumors formed efficiently (Fig. 2*A*). Similar observations were made when the cells were injected s.c. into nude mice (data not shown). These tumors developed as fast as tumors generated by MYC/Ha-RAS–transformed REFs (data not shown). However, histologic analyses identified differences between tumors derived from MYC/Ha-RAS– and hASH2/Ha-RAS–transformed cells (Fig. 2*B*). MYC/Ha-RAS tumors were characterized by high cell density and storiform appearance as seen in low-grade differentiated sarcoma (Fig. 2*B, left*). In contrast, hASH2/Ha-RAS tumors were less dense, and the cells were disorganized comparable with a grade 3 sarcoma (Fig. 2*B, right*). These tumors frequently showed necrotic areas not seen in MYC/Ha-RAS tumors (Fig. 2*B, arrowheads*) and many mitotic figures, suggesting a high proliferative potential (Fig. 2*C*). About half of the mitotic cells were characterized by a ring-like chromatin organization, indicative of multiple centrosomes (Fig. 2*C, arrows* and *inset*). Portions of the hASH2/Ha-RAS tumors were explanted and readily established new lines in culture (data not shown). The two initial lines, AR-925 and AR-932, as well as the lines established from the tumors expressed hASH2 as determined by Western blotting (Fig. 2*D*). Together, these findings suggest that REFs transformed *in vitro* by hASH2 and Ha-RAS were highly malignant in animals.

***hASH2* gene expression is not deregulated in human tumors.** The findings described above suggested that hASH2 might function as an oncoprotein in human tumors. Therefore, we addressed whether the expression of the *hASH2* gene, which is ubiquitously expressed in normal tissues (Fig. 3*A*), is deregulated in human malignancies. We probed a cancer array with a cDNA specific for *hASH2* (Fig. 3*B*). Very little variation in *hASH2* expression, compared with *glyceraldehyde-3-phosphate dehydrogenase* (*GAPDH*; data not shown), was observed in a broad set of tumors of different origin and corresponding normal tissue, and in several tumor cell lines. To validate this finding, we measured *hASH2* mRNA levels in human cell lines and primary cells by Northern blotting. With few exceptions, comparable *hASH2* expression was observed (Fig. 3*C*; Table 1). Increased *hASH2* mRNA was seen in only in 3 of 26 mammary carcinoma cell lines, BT483, MDA-MB134VI, and MFM223, compared with primary cells. This finding was verified by quantitative reverse transcription-PCR (RT-PCR; Fig. 3*D*; Table 1).

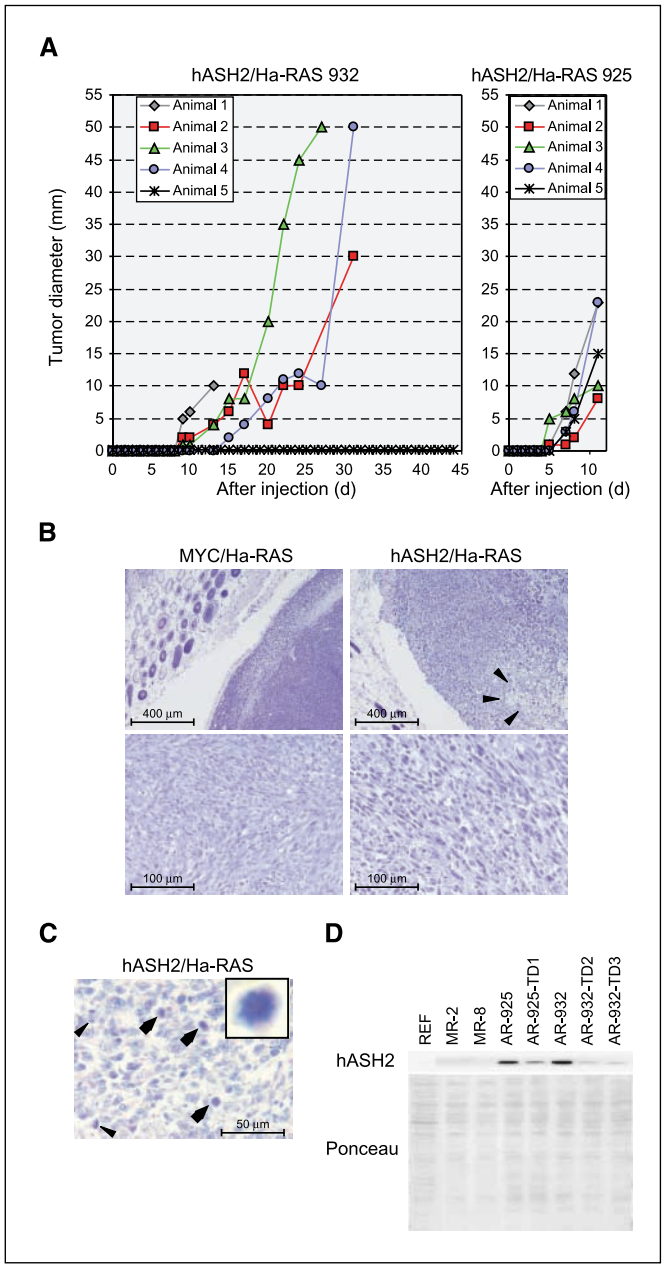

Figure 2. hASH2/Ha-RAS–transformed REFs are tumorigenic in animals. *A,* two cell lines, hASH2/Ha-RAS-925 and hASH2/Ha-RAS-932, were established from hASH2/Ha-RAS–transformed foci. Seven- to 10-d-old, syngeneic male rats were injected s.c. with 5×10^4 early passage AR-932 and AR-925 cells. Five animals were injected with each of the two lines. Tumor size was monitored regularly. In all but one animal, tumors rapidly developed. The tumor diameters are shown for each animal over time. When the tumors became large or were developing at unfavorable location, the animals were killed to prevent discomfort. *B,* histologic analysis of tumors derived from animals injected with MYC/Ha-RAS– or hASH2/Ha-RAS–transformed cells. H&E stainings are shown in low magnification (*top*). *Arrowheads,* necrotic zone of the hASH2/Ha-RAS tumor. *Bottom,* higher magnification pictures. Note the storiform, structured appearance of the cells in the MYC/Ha-RAS tumor, whereas the hASH2/Ha-RAS tumor shows a high degree of disorganization. *C,* a high magnification of a section of a hASH2/Ha-RAS tumor. Of note is the high percentage of mitotic figures in sections of these tumors. *Arrowheads,* mitotic cells; *arrows,* mitotic cells that show ring-like organization of the spindle, an indication for multiple centrosomes. *Inset,* an enlarged mitotic cell with a ring-like organization of condensed chromatin. *D,* the expression of hASH2 in REFs and different transformed REF cell lines is shown by Western blot analysis using mAb 4C5. The Ponceau-stained filter of the total cell lysates before immunodetection is shown to demonstrate equal loading of cell extracts.

Finally, we determined *hASH2* mRNA levels in primary tumors. Malignant and corresponding normal tissue samples were obtained by microdissection. In general, *hASH2* mRNA expression was comparable between normal and tumor tissue (Fig. 3*D*). In summary, with a few exceptions, *hASH2* mRNA expression was within a 2-fold range compared with exponentially growing HDFs and HMECs. This rather uniform expression was unexpected in light of the transforming ability of hASH2 when expressed ectopically. Therefore, we reverse transcribed, amplified, and sequenced 2,360-bp *hASH2* RNA of two primary cultures, nine mammary carcinoma cell lines, and one spontaneously immortalized mammary epithelial cell line. All 12 sequences were identical to the National Center for Biotechnology Information (NCBI) reference sequence NM 004674 (data not shown; summarized in Table 1). Together, these findings indicate that *hASH2* is neither deregulated nor mutated in human tumors.

hASH2 protein expression is elevated in human tumors. We then considered that the expression of hASH2 protein might be distinct between normal and malignant cells, possibly controlled at a posttranscriptional level. Western blot analysis of total cell extracts of transformed cell lines and of nontransformed primary cells revealed that malignant cells in general had increased levels of hASH2 protein (Fig. 4*A, left*; Table 1). For these studies, several mAbs and two polyclonal rabbit sera were developed that recognized hASH2 specifically (data not shown). Similar to the findings with cell lines, more hASH2 was detectable in tumor samples compared with normal tissue (Fig. 4*A, right*). We then measured hASH2 expression in tumor biopsies upon microdissection. In general, hASH2 protein levels were higher in the material derived from areas with a high load of malignant cells compared with areas with primarily normal cells as determined by visual inspection of H&E-stained sections of the biopsies (Fig. 4*B*). However, in most instances, *hASH2* mRNA levels from the same biopsies were not enhanced compared with controls using quantitative RT-PCR analysis. Furthermore, immunohistochemical analysis showed that, in general, malignant cells stained strongly for hASH2, as shown here for a renal cell carcinoma (Fig. 4*B*). This staining was nuclear as seen in all other tumors and normal samples analyzed (Fig. 4*C* and *D*), which is also in agreement with immunofluorescence studies of transiently expressed as well as endogenous hASH2 in tissue culture cells (data not shown). The cells in the glomerulus of a normal kidney section were only weakly positive, whereas the connective tissue fibroblasts were mostly negative. Furthermore, the endothelial tubular cells showed weak, most likely unspecific staining in the cytoplasm (Fig. 4*B, bottom*). These findings are consistent with hASH2 expression being enhanced in another renal cell carcinoma and lower but detectable expression in normal kidney tissue (Fig. 4*A, right*).

To evaluate the expression of hASH2 in tumor cells in more detail, different tumor entities were stained for hASH2 and compared with the corresponding normal tissue (Fig. 4*C* and *D*). In general, all tumors analyzed of a wide spectrum showed robust nuclear staining for hASH2. This is exemplified for squamous cell carcinoma of the cervix and larynx and for melanoma, in which virtually all tumor cells are positive (Fig. 4*C*). In the matching normal tissues, a weakening of hASH2 staining was seen toward the apical epithelial areas. Superficial cell layers in the normal squamous epithelium presented a weak or negative reaction, suggesting that in these tissues, hASH2 expression was reduced upon differentiation. The connective tissue below the basal cell layer revealed fibroblasts with weak or no staining and focally

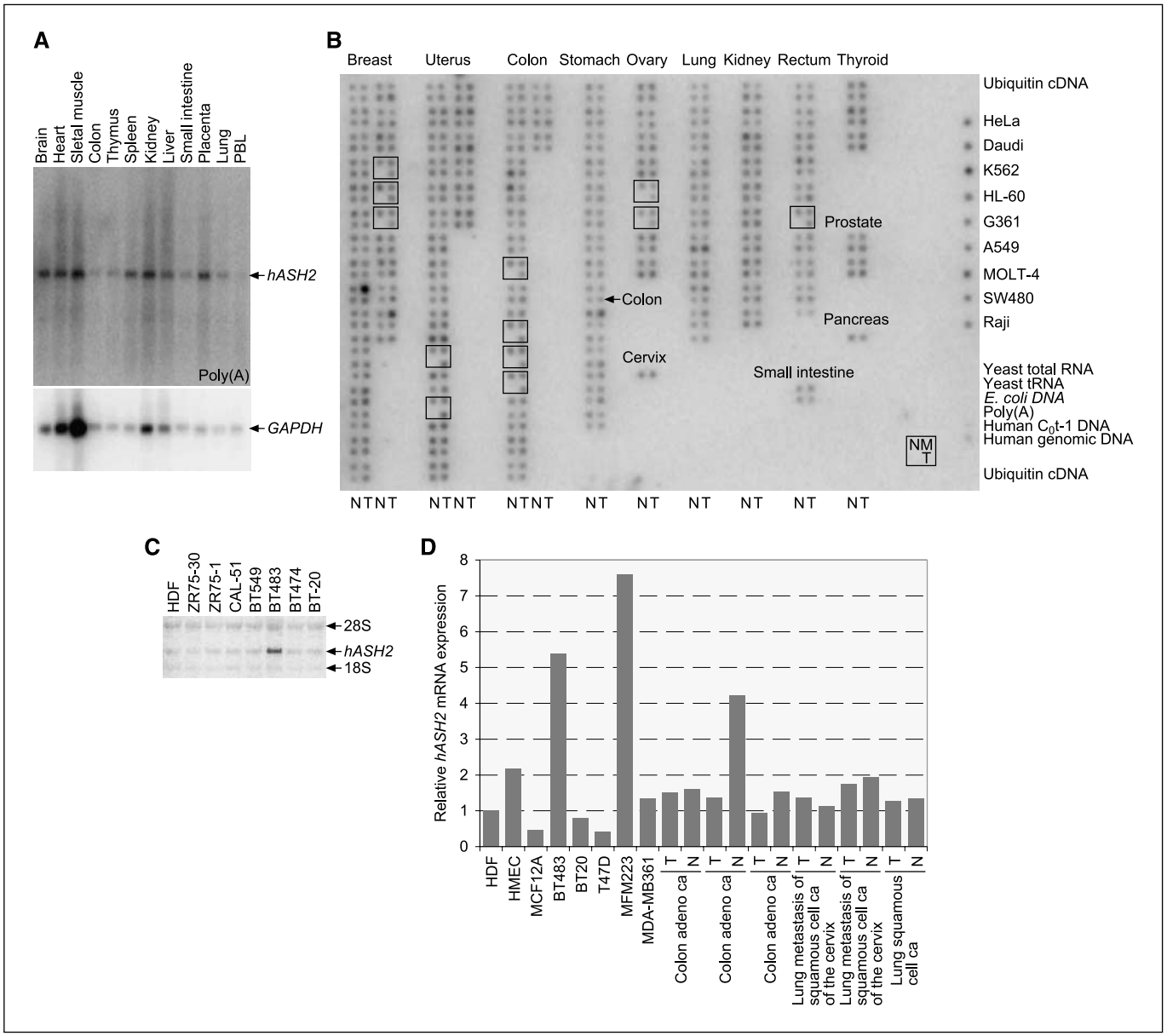

Figure 3. *hASH2* mRNA expression is not deregulated in human tumors. *A,* a commercially available multitissue Northern blot was probed with an *hASH2* cDNA. A single mRNA species of about 2.36 kb was detected (*top*). For control, the blot was developed with a *GAPDH* probe (*bottom*). *B,* a commercially available cancer profiling array was probed with an *hASH2* cDNA. The tissues analyzed and the cDNAs of tumors (*T*) and of the corresponding normal tissues (*N*) are indicated. For some samples, in addition to cDNAs of tumor and normal tissue, cDNA of a metastasis (*M*) is spotted as indicated (*bottom right hand corner*). For control, cDNAs of different cell lines and RNA or DNA of different origin are spotted as indicated (*to the right of the filter*). *C,* total RNA of the indicated cell lines was analyzed by Northern blotting using an *hASH2* cDNA. For control, the weak cross-reactivity to 18S and 28S rRNA is shown. *D,* quantitative RT-PCR analysis of *hASH2* expression in different cell lines and in tumor, and corresponding normal tissue. The reactions were standardized for β-glucuronidase expression. The signal from primary HDF was artificially set as 1. BT483 and MFM223 were selected from a total of 26 breast carcinoma (*ca*) cell lines because Northern blot analysis revealed increased *hASH2* mRNA levels in both lines.

strongly stained lymphocytes (Fig. 4*C*). In addition, the tumor cells of a rhabdomyosarcoma showed strong nuclear staining, whereas the matching normal skeletal muscle was almost negative (Fig. 4*C*). Robust staining of tumor cell nuclei was also detected in an adenocarcinoma of the pancreas (Fig. 4*C*). Normal pancreas showed intermediate reactivity in all acinar cells, whereas ductal cells were less positive (Fig. 4*C*). Furthermore, strong nuclear staining for hASH2 was present in cells of breast and colon carcinomas (Fig. 4*D*). Normal breast tissue also exhibited strong nuclear staining in the acini. Normal colon epithelium was generally strongly nuclear positive in goblet cells but showed a slight weakening in nuclei of cells located more apically in the crypts. The surrounding connective tissue was weakly positive with the exception of substantially stained lymphocytes (Fig. 4*D*). These examples are from a selection of >200 different tumor samples analyzed. In all cases, tumor cells were positive for hASH2. It is important to note that many normal cells also stained positive, indicating that the expression of hASH2 is not exclusive to tumor cells. Nevertheless, the expression of hASH2 was frequently elevated in tumor cells compared with the corresponding normal cells.

Table 1. Summary of *hAHS2* mRNA and protein expression and cDNA sequences in different human cell lines and primary cell cultures

Cells	Origin	*hASH2* mRNA levels (Northern/real-time PCR)*	hASH2 protein levels (steady state)	*hASH2* cDNA sequence †
HDF	Human diploid fibroblasts	+/+	+	Wild-type
HMEC	Human mammary epithelial cells	ND/+	+	Wild-type
PBMC	Peripheral blood mononuclear cells	ND/ND	+	ND
BT20	Mamma adenocarcinoma	+/+	+	ND
BT474	Mamma ductal carcinoma	+/+	+++	Wild-type
BT483	Mamma ductal carcinoma	++/++	+++	Wild-type
BT549	Mamma ductal carcinoma	+/ND	+	ND
CAL-51	Mamma adenocarcinoma	+/ND	++	ND
ZR75-1	Mamma ductal carcinoma	+/ND	++	ND
ZR75-30	Mamma ductal carcinoma	+/ND	+	ND
EFM19	Mamma adenocarcinoma	+/ND	++	Wild-type
EFM192A	Mamma adenocarcinoma	+/ND	++	Wild-type
EFM192B	Mamma adenocarcinoma	+/ND	++	ND
EFM192C	Mamma adenocarcinoma	+/ND	+	ND
HS578T	Mamma carcinoma	+/ND	+	ND
T47D	Mamma ductal carcinoma	+/+	++	Wild-type
MFM223	Mamma carcinoma	++/++	+++	Wild-type
MDA-MB134VI	Mamma ductal carcinoma	++/ND	+++	Wild-type
MDA-MB361	Mamma ductal carcinoma	+/+	ND	Wild-type
MDA-MB415	Mamma adenocarcinoma	+/ND	++	ND
MDA-MB435s	Mamma ductal carcinoma	+/ND	++	ND
MDA-MB436	Mamma adenocarcinoma	ND/ND	+	ND
MDA-MB453	Mamma carcinoma	+/ND	++	ND
MDA-MB468	Mamma adenocarcinoma	+/ND	++	ND
KPL-1	Mamma ductal carcinoma	+/ND	ND	ND
UAC-812	Mamma ductal carcinoma	+/ND	++	ND
UAC-893	Mamma ductal carcinoma	+/ND	++	ND
HBL-100	From breast milk, contains SV40	+/ND	ND	Wild-type
SK-BR3	Mamma adenocarcinoma	+/ND	++	ND
MCF7	Mamma carcinoma	+/ND	++	ND
MCF12a	From reduction mammoplasty, spontaneously immortalized	+/+	+	Wild-type
HeLa	Cervical carcinoma	+/ND	++	ND
HEK293	Human epithelial kidney derived, contains adenoviral DNA	ND/+	++	ND
U2OS	Osteosarcoma	ND/ND	++	ND
SAOS2	Osteosarcoma	ND/ND	++	ND
Jurkat	T cell lymphoma	+/ND	+	ND
Manca	Burkitt's lymphoma	ND/ND	+	ND
Nawalma	Burkitt's lymphoma	ND/ND	+	ND
CA46	Burkitt's lymphoma	ND/ND	++	ND
Ramos	Burkitt's lymphoma	ND/ND	+	ND
U937	Promyelocytic leukemia	ND/ND	++	ND
HL60	Promyelocytic leukemia	+/ND	++	ND

Abbreviation: ND, not determined.

*See also *hASH2* expression in additional cell lines that were used for control on the cancer array (Fig. 3*B*).

†The 2,360-bp cDNAs of *hASH2* were amplified using PCR from the indicated primary cells and cell lines, and sequenced. All 12 sequences were identical to the NCBI reference sequence NM 004674.

hASH2 is necessary for cell proliferation. Because the majority of the cell lines have *hASH2* mRNA levels that are comparable with primary cells, i.e., cultivated HDF and mammary epithelial cells and freshly prepared peripheral mononuclear cells (Fig. 3; Table 1), but distinct proteins levels (Fig. 4), we addressed whether the stability of hASH2 protein was altered. [^{35}S]methionine pulse chase analysis showed that hASH2 is a rather stable protein. Whereas in primary HDF, a decrease in labeled hASH2 was detectable after a chase of 20 h, the protein was very stable with only a small decrease in hASH2-associated radioactivity in the BT474 breast cancer cell line (Fig. 5*A*). In addition, we noticed that significantly more [^{35}S]methionine-labeled hASH2 was immunoprecipitated from extracts of BT474 compared with HDF cells containing equal amounts of metabolically pulse-labeled proteins

(Fig. 5*A, inset*). Thus, in the tumor cell line BT474, hASH2 was more stable and synthesized more efficiently than in HDF cells, the latter despite the observation that *hASH2* mRNA levels were identical (Fig. 3*C*; Table 1). It is likely that these distinct effects on synthesis and stability contribute to the observed differences in the steady-state levels of hASH2 between tumor and primary cells.

Next, we addressed the role of hASH2 for tumor cell proliferation. In HeLa, U2OS, and HEK293 tumor cells, the knockdown of hASH2 resulted in reduced protein expression as seen by immunohistochemistry and Western blotting (Fig. 5*B* and data not shown). To evaluate proliferation, HeLa and U2OS cells were cotransfected with siRNA-expressing vectors and with a plasmid encoding a puromycin resistance marker (pBABE-puro) that

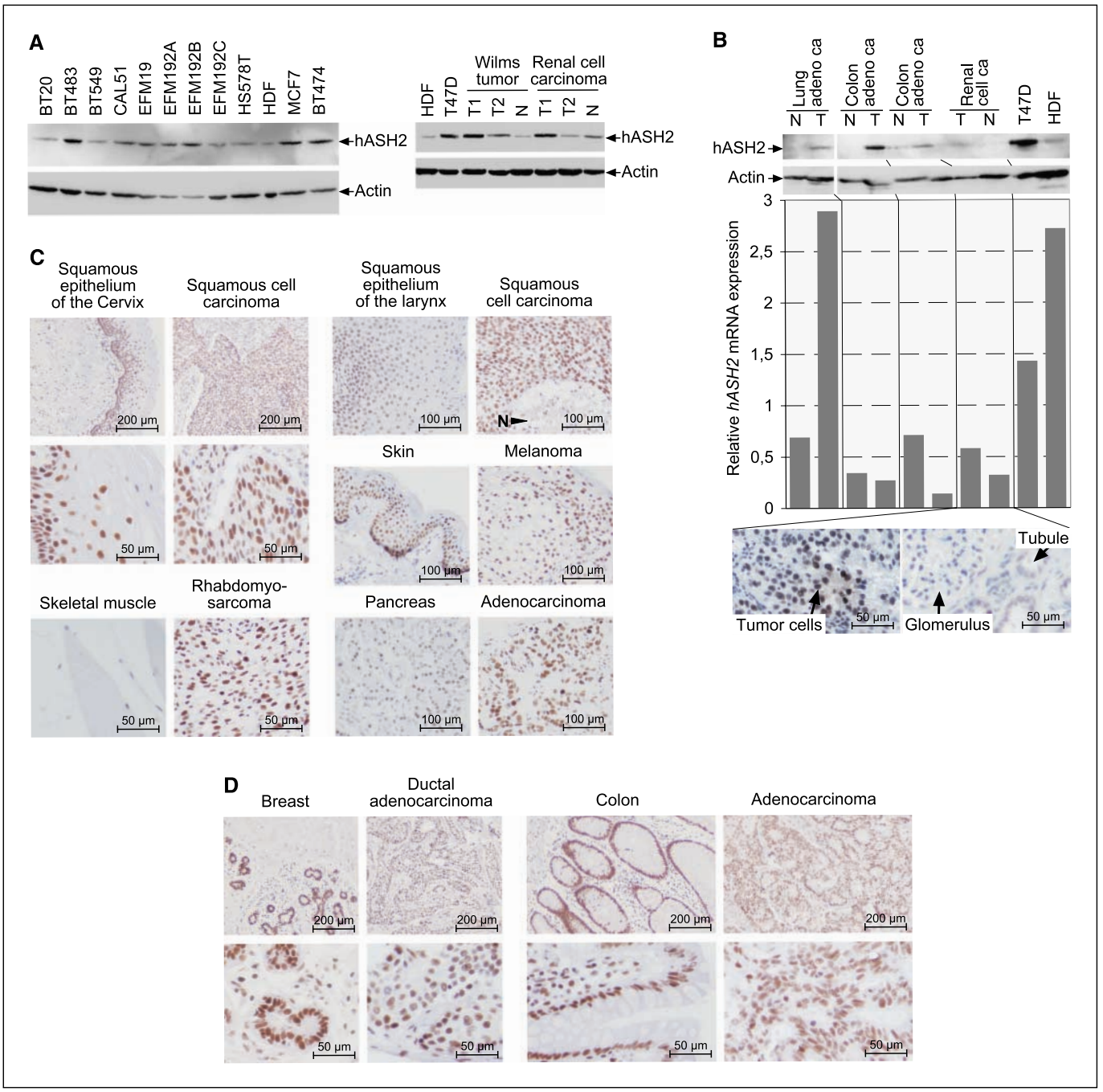

Figure 4. Increased hASH2 protein expression in human tumors. *A,* total cell lysates of different tumor cell lines and primary cells were prepared, and equal amounts of proteins were analyzed by Western blotting. In addition, tissue from two tumors (*T1* and *T2* refer to two different locations of the same tumor) and the corresponding normal tissue were analyzed for ASH2 expression. For hASH2, mAb 4C5 was used. For control, the blots were developed with an antibody specific for actin. *B,* tumor and normal tissue from the same biopsy were prepared, and protein and RNA were extracted. Proteins were analyzed by Western blotting as described in *A*. For comparison, lysates of HDF and of T47D mammary carcinoma cells were used. *Middle,* the quantification of *hASH2* mRNA by quantitative RT-PCR. *β-glucuronidase* served as internal standard. *Bottom,* immunohistochemical staining of hASH2 of a kidney carcinoma (renal cell; *left*) and normal kidney (*right*) from the same biopsy using mAb 4C5. *C* and *D,* immunohistochemistry of the indicated normal and tumor tissues using mAb 4C5 and 6A9.

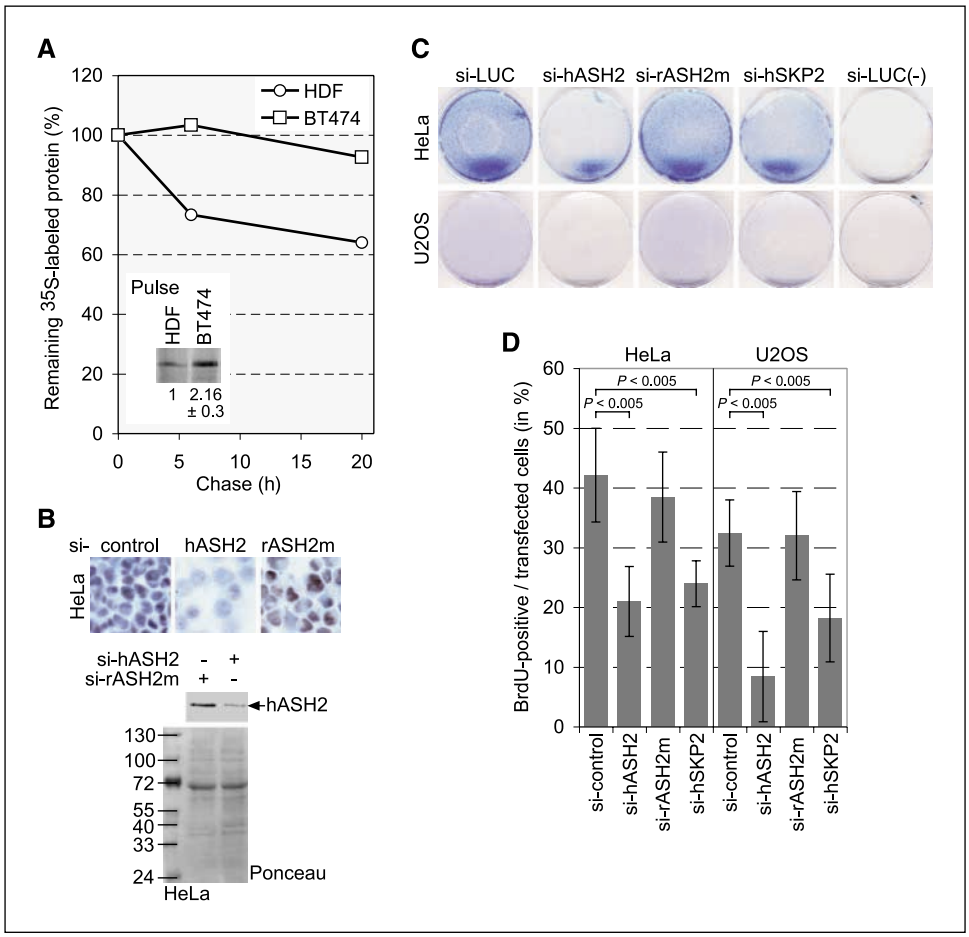

Figure 5. Regulation of hASH2 protein expression and relevance for tumor cell proliferation. *A,* HDF and BT474 cells were metabolically labeled with [^{35}S]methionine for 30 min and then chased with excess unlabeled methionine for the indicated times. The incorporated radioactivity was determined for each cell lysate, and aliquots of these lysates with equal amounts of radioactivity were used for hASH2-specific immunoprecipitations. The radioactivity associated with hASH2 was then measured, and the relative amounts are blotted. *Inset,* [^{35}S]methionine pulse-labeled, immunoprecipitated hASH2 is shown. The relative labeling of hASH2 in HDF and BT474 cells is given from four independent experiments. *B,* pSUPER constructs expressing the indicated siRNAs were transfected into HeLa cells together with a pEGFP control plasmid. Transfection efficiency was about 80% as determined by green fluorescent protein fluorescence (data not shown). The transfected cells were embedded in paraffin, and then hASH2 expression was analyzed immunohistochemically using mAb 4C5 (*top*). In addition, the transfected cells were lysed in Frackelton buffer, and the expression of hASH2 was examined by Western blotting using mAb 4C5. For control, the Ponceau-stained blot is shown. *C,* HeLa and U2OS cells were transfected with pSUPER constructs expressing the indicated siRNAs. In addition, pBABE-puro was cotransfected, except for the plates shown on the right [si-LUC(−)]. The cells were selected on puromycin for 24 h, replated, and stained after 4 d. *D,* HeLa and U2OS cells were transfected with pSUPER constructs expressing the indicated siRNAs and with pEGFP. After 72 h, the cells were pulse-labeled with BrdUrd for 1 h. The number of BrdUrd-positive cells of the transfected cells was determined. *Columns,* mean values of three independent experiments with >100 cells analyzed per experiment; *bars,* SD.

allowed selecting the transfected cells with puromycin. Reducing hASH2 levels inhibited proliferation of the transfected cells in both lines, whereas si-rASH2m or an siRNA specific for luciferase had no effect (Fig. 5*C*). These effects were at least as strong as knockdown of hSKP2. This protein mediates degradation of the cyclin-dependent kinase inhibitor $p27^{KIP1}$ at the G_1-S phase transition, and its knockdown inhibits proliferation (40). In the absence of pBABE-puro, no cells survived the puromycin selection. Furthermore, we determined the effect of the hASH2 knockdown on the ability of cells to enter S phase. Repression of hASH2 reduced S-phase progression in HeLa and U2OS cells as determined by measuring the incorporation of BrdUrd (Fig. 5*D*). In this assay, the effect was comparable with the one elicited by the knockdown of hSKP2. As for the proliferation assay, si-rASH2m was ineffective. We concluded from these studies that hASH2 overexpression provides tumor cells with a growth advantage.

Discussion

In this report, we provide evidence that the trithorax protein ASH2 functions as an oncoprotein. This conclusion is based on the findings that hASH2 cooperates with Ha-RAS in the transformation of REFs, that hASH2 is overexpressed in human tumors, and that the knockdown of hASH2 results in the inhibition of proliferation of tumor cell lines. Importantly, the overexpression of hASH2 is due to increased protein synthesis and stability in tumor cells and not due to deregulated expression of the gene.

hASH2 has been found in at least four human complexes that possess HMT activity. These complexes have distinct protein compositions with different catalytic subunits that can specifically trimethylate H3K4 (21, 23). This histone mark is closely associated with promoters of actively transcribed genes (25, 27). Of particular interest are the findings that two of these HMT complexes contain the tumor suppressor Menin and either MLL1 or MLL4 as the catalytic subunits (15, 18, 20, 42, 43). MLL proteins function as

oncoproteins in a number of distinct human tumors. The *MLL1* gene is translocated in and associated with aggressive acute leukemias, whereas *MLL4* is amplified in some solid tumors (44). Menin is the product of the tumor suppressor gene *MEN1* (43). Loss of function mutations of *MEN1* are observed in sporadic and heritable endocrine tumors (42). Thus, with MLL and Menin, these complexes contain both a tumor suppressor protein and an oncoprotein. Our data now provide evidence for an additional subunit, ASH2, associated with these complexes that is involved in tumorigenesis. Although MLL1, MLL4, and Menin are associated with specific tumors, our data suggest that increased hASH2 expression is very broadly associated with tumor formation. Together, these findings strongly indicate that the ASH2/MLL/Menin complexes are tied closely to tumor formation in many different cell types.

Because these complexes are involved in chromatin regulation, it seems likely that the deregulation of any of these proteins is associated with altered gene transcription. Indeed, MLLs have been linked to the expression of *HOX* and *CDK inhibitor* genes. Deregulation of these seems to be relevant for tumor formation (18, 45–47). The molecular function of Menin is less well understood. It has been suggested that the HMT activity of MLL4 is dependent on Menin (43). The molecular role of AHS2 is poorly understood. Knockdown of ASH2 results in a reduction of trimethylation of H3K4 (21),[5] suggesting that this protein is important for the activity of the HMT complexes. This might result in the deregulation of many genes and possibly explains the reduced proliferation in response to the ASH2 knockdown (Fig. 5). It is conceivable that ASH2 is important to allow complex formation and/or to stabilize the MLL complex (21). Additionally, ASH2 might target the MLL complexes to specific promoters by interacting with transcriptional regulators or other chromatin-bound proteins. In support, ASH2 directly binds to the oncoprotein MYC.[5] It will now be important to define the molecular functions of ASH2 in more detail. Together, the findings presented here and the published observations strongly suggest that the ASH2/MLL/Menin complexes affect cell transformation by controlling gene expression.

[5] Our own unpublished findings.

Acknowledgments

Received 8/16/2007; revised 10/22/2007; accepted 11/26/2007.

Grant support: Interdisciplinary Centre for Clinical Research "BIOMAT" within the faculty of Medicine at the RWTH Aachen University (TV M1) and the Deutsche Forschungsgemeinschaft DFG (B. Lüscher).

The costs of publication of this article were defrayed in part by the payment of page charges. This article must therefore be hereby marked *advertisement* in accordance with 18 U.S.C. Section 1734 solely to indicate this fact.

We thank R. Kraft and M. Austen for microsequencing the p86 protein band, E. Dahl for providing the Cancer Profiling Array filter, G. Evan and R. Bernards for the expression vectors, J. Baron for the human diploid fibroblasts, and D. Smeets and J. Stahl for expert technical assistance.

References

1. Hanahan D, Weinberg RA. The hallmarks of cancer. Cell 2000;100:57–70.
2. Guo QM. DNA microarray and cancer. Curr Opin Oncol 2003;15:36–43.
3. Pinkel D, Albertson DG. Array comparative genomic hybridization and its applications in cancer. Nat Genet 2005;37 Suppl:S11–7.
4. Downward J. Targeting RAS signalling pathways in cancer therapy. Nat Rev Cancer 2003;3:11–22.
5. Koff A. How to decrease p27Kip1 levels during tumor development. Cancer Cell 2006;9:75–6.
6. Orlando V, Paro R. Chromatin multiprotein complexes involved in the maintenance of transcription patterns. Curr Opin Genet Dev 1995;5:174–9.
7. Ringrose L, Paro R. Epigenetic regulation of cellular memory by the Polycomb and Trithorax group proteins. Annu Rev Genet 2004;38:413–43.
8. Schwartz YB, Pirrotta V. Polycomb silencing mechanisms and the management of genomic programmes. Nat Rev Genet 2007;8:9–22.
9. Shearn A, Rice T, Garen A, Gehring W. Imaginal disc abnormalities in lethal mutants of *Drosophila*. Proc Natl Acad Sci U S A 1971;68:2594–8.
10. Adamson AL, Shearn A. Molecular genetic analysis of *Drosophila* ash2, a member of the trithorax group required for imaginal disc pattern formation. Genetics 1996;144:621–33.
11. LaJeunesse D, Shearn A. Trans-regulation of thoracic homeotic selector genes of the Antennapedia and bithorax complexes by the trithorax group genes: absent, small, and homeotic discs 1 and 2. Mech Dev 1995;53:123–39.
12. Beltran S, Angulo M, Pignatelli M, Serras F, Corominas M. Functional dissection of the ash2 and ash1 transcriptomes provides insights into the transcriptional basis of wing phenotypes and reveals conserved protein interactions. Genome Biol 2007;8:R67.
13. Beltran S, Blanco E, Serras F, et al. Transcriptional network controlled by the trithorax-group gene ash2 in *Drosophila melanogaster*. Proc Natl Acad Sci U S A 2003; 100:3293–8.
14. Goo YH, Sohn YC, Kim DH, et al. Activating signal cointegrator 2 belongs to a novel steady-state complex that contains a subset of trithorax group proteins. Mol Cell Biol 2003;23:140–9.
15. Hughes CM, Rozenblatt-Rosen O, Milne TA, et al. Menin associates with a trithorax family histone methyltransferase complex and with the hoxc8 locus. Mol Cell 2004;13:587–97.
16. Lee JH, Skalnik DG. CpG-binding protein (CXXC finger protein 1) is a component of the mammalian Set1 histone H3–4 methyltransferase complex, the analogue of the yeast Set1/COMPASS complex. J Biol Chem 2005; 280:41725–31.
17. Miller T, Krogan NJ, Dover J, et al. COMPASS: a complex of proteins associated with a trithorax-related SET domain protein. Proc Natl Acad Sci U S A 2001;98: 12902–7.
18. Milne TA, Hughes CM, Lloyd R, et al. Menin and MLL cooperatively regulate expression of cyclin-dependent kinase inhibitors. Proc Natl Acad Sci U S A 2005;102: 749–54.
19. Wysocka J, Myers MP, Laherty CD, Eisenman RN, Herr W. Human Sin3 deacetylase and trithorax-related Set1/Ash2 histone H3-4 methyltransferase are tethered together selectively by the cell-proliferation factor HCF-1. Genes Dev 2003;17:896–911.
20. Yokoyama A, Wang Z, Wysocka J, et al. Leukemia proto-oncoprotein MLL forms a SET1-like histone methyltransferase complex with menin to regulate Hox gene expression. Mol Cell Biol 2004;24:5639–49.
21. Dou Y, Milne TA, Ruthenburg AJ, et al. Regulation of MLL1 H3K4 methyltransferase activity by its core components. Nat Struct Mol Biol 2006;13:713–9.
22. Guccione E, Bassi C, Casadio F, et al. Methylation of histone H3R2 by PRMT6 and H3K4 by an MLL complex are mutually exclusive. Nature 2007;449:933–7.
23. Steward MM, Lee JS, O'Donovan A, et al. Molecular regulation of H3K4 trimethylation by ASH2L, a shared subunit of MLL complexes. Nat Struct Mol Biol 2006;13: 852–4.
24. Berger SL. The complex language of chromatin regulation during transcription. Nature 2007;447: 407–12.
25. Li B, Carey M, Workman JL. The role of chromatin during transcription. Cell 2007;128:707–19.
26. Cosgrove MS, Wolberger C. How does the histone code work? Biochem Cell Biol 2005;83:468–76.
27. Ruthenburg AJ, Allis CD, Wysocka J. Methylation of lysine 4 on histone H3: intricacy of writing and reading a single epigenetic mark. Mol Cell 2007;25: 15–30.
28. Bernstein BE, Kamal M, Lindblad-Toh K, et al. Genomic maps and comparative analysis of histone modifications in human and mouse. Cell 2005;120: 169–81.
29. Ng HH, Robert F, Young RA, Struhl K. Targeted recruitment of Set1 histone methylase by elongating Pol II provides a localized mark and memory of recent transcriptional activity. Mol Cell 2003;11:709–19.
30. Santos-Rosa H, Schneider R, Bannister AJ, et al. Active genes are tri-methylated at K4 of histone H3. Nature 2002;419:407–11.
31. Schneider R, Bannister AJ, Myers FA, et al. Histone H3 lysine 4 methylation patterns in higher eukaryotic genes. Nat Cell Biol 2004;6:73–7.
32. Schubeler D, MacAlpine DM, Scalzo D, et al. The histone modification pattern of active genes revealed through genome-wide chromatin analysis of a higher eukaryote. Genes Dev 2004;18:1263–71.
33. Shi X, Gozani O. The fellowships of the INGs. J Cell Biochem 2005;96:1127–36.
34. Vermeulen M, Mulder KW, Denissov S, et al. Selective anchoring of TFIID to nucleosomes by trimethylation of histone H3 lysine 4. Cell 2007;131:58–69.
35. Shi Y, Whetstine JR. Dynamic regulation of histone lysine methylation by demethylases. Mol Cell 2007;25:1–14.
36. Yu M, Schreek S, Cerni C, et al. PARP-10, a novel Myc-interacting protein with poly(ADP-ribose) polymerase

activity, inhibits transformation. Oncogene 2005;24:1982–93.
37. Land H, Parada LF, Weinberg RA. Tumorigenic conversion of primary embryo fibroblasts requires at least two cooperating oncogenes. Nature 1983;304:596–602.
38. Cerni C, Bousset K, Seelos C, et al. Differential effects by Mad and Max on transformation by cellular and viral oncoproteins. Oncogene 1995;11:587–96.
39. Brummelkamp TR, Bernards R, Agami R. A system for stable expression of short interfering RNAs in mammalian cells. Science 2002;296:550–3.
40. Garriga J, Bhattacharya S, Calbo J, et al. CDK9 is constitutively expressed throughout the cell cycle, and its steady-state expression is independent of SKP2. Mol Cell Biol 2003;23:5165–73.
41. Sommer A, Bousset K, Kremmer E, Austen M, Luscher B. Identification and characterization of specific DNA-binding complexes containing members of the Myc/Max/Mad network of transcriptional regulators. J Biol Chem 1998;273:6632–42.
42. Chandrasekharappa SC, Teh BT. Functional studies of the MEN1 gene. J Intern Med 2003;253:606–15.
43. Yokoyama A, Somervaille TC, Smith KS, et al. The menin tumor suppressor protein is an essential oncogenic cofactor for MLL-associated leukemogenesis. Cell 2005;123:207–18.
44. Hess JL. Mechanisms of transformation by MLL. Crit Rev Eukaryot Gene Expr 2004;14:235–54.
45. Ayton PM, Cleary ML. Transformation of myeloid progenitors by MLL oncoproteins is dependent on Hoxa7 and Hoxa9. Genes Dev 2003;17:2298–307.
46. Karnik SK, Hughes CM, Gu X, et al. Menin regulates pancreatic islet growth by promoting histone methylation and expression of genes encoding p27Kip1 and p18INK4c. Proc Natl Acad Sci U S A 2005;102:14659–64.
47. Zeisig BB, Milne T, Garcia-Cuellar MP, et al. Hoxa9 and Meis1 are key targets for MLL-ENL-mediated cellular immortalization. Mol Cell Biol 2004;24:617–28.

The Human Trithorax Protein hASH2 Functions as an Oncoprotein

Juliane Lüscher-Firzlaff, Isabella Gawlista, Jörg Vervoorts, et al.

Cancer Res 2008;68:749-758.